Sensors and Materials, Vol. 37, No. 12 (2025) 5385–5398
MYU Tokyo

S & M 4251

Intruder Detection System in an Entrance Area Using Ultrasonic Technology

Přemysl Janů[1*] and Antonín Kučera[2]

[1]Department of Aviation Technology, Faculty of Military Technology, University of Defence, Kounicova 65, 662 10, Brno, Czech Republic
[2]Operational Analysis Workplace at Passive Surveillance System Company, Czech Army Ground Forces, Kpt. Jaroše 3, 390 03, Tábor, Czech Republic

(Received September 11, 2025; accepted October 30, 2025)

Keywords: electronic security systems, intruder, ultrasonic technology, piezoelectric ceramic transducer, microprocessor system

The study is devoted to the complete design, assembly, and detailed verification of the functionality of the barrier based on ultrasonic technology for the detection of different intruders in an entrance area. This barrier is used in the perimeter and shell protection of guarded areas. The construction of the barrier, the selection of the most suitable sensors, the design of the transmitting and receiving parts, analog and digital processing, a modern microprocessor system, and the complete assembly and testing of the system's response to various types of intruder are accurately described here. The system can not only evaluate the intruder presence, but also determine the type, such as a person, child, animal, and flying object, which gives the barrier a certain intelligence. Economical and easily available components on the market, as well as modern electronic devices, are chosen in the design. Directly, the microprocessor system allows the communication and transmission of the information about the character of the intruder, not only via universal serial bus but also via several wireless technologies. These technologies are Bluetooth, Bluetooth low energy, and also Wi-Fi. With these technologies, the algorithm in the microprocessor system can also be modified. The designed device represents a certain prototype that can be improved in the future with increasingly modern technologies.

1. Introduction

Nowadays, ultrasonic technology is used in various fields and areas of human activity. This is primarily due to the relatively low economic demands of this technology. It plays an important role in the health sector in the analysis of the properties of individual tissues.[1–5] Furthermore, in the field of nondestructive defectoscopy, ultrasonic technology is used.[6–11] The acoustic ultrasonic signal has also found its place in industry, particularly the automotive industry, communication technologies, and robotics, especially in unmanned vehicles.[12–18]

The most widespread application of ultrasonic technology is the measurement of the time of flight of the acoustic signal from the transmitting transducer back to the receiving transducer,

*Corresponding author: e-mail: premysl.janu@unob.cz
https://doi.org/10.18494/SAM5935

ISSN 0914-4935

from which other parameters can subsequently be derived, such as the distance to the obstacle, the height of the flight of the unmanned vehicle above the terrain during the landing phase, and the amount of fuel in a tank.[19–22]

As a key technology in the field of intruder detection in electronic security systems, ultrasound is not very common.[23–25] Various systems are used to detect an intruder in a guarded area, such as passive infrared detectors, microwave detectors, infrared bars, barriers, curtains, and significantly expanded camera systems, which are more economically demanding.[26,27] Thus, this study is dedicated to the detection of an intruder in the entrance area using ultrasonic technology. In this case, ultrasonic technology is applied in the form of a barrier. The ultrasonic signal travels from the transmitter to the receiver and, when an intruder is present, that signal is interrupted. The signal voltage level on the receiving side is 0 V. The evaluation of the time of flight of the acoustic ultrasonic signal is not addressed here, and therefore, the processing of the signal is not very demanding. Barrier detectors are mainly used in shield or perimeter protection systems. These systems detect intruders (unwanted persons or animals) through any passage in the building or the perimeter of the building (doors, windows, gates, gateways, or other free passages).

Janů and Odvárková already presented the detailed design and testing of the intelligent ultrasonic barrier in the application of guarding the entrance to the building through the door.[28] The following sections show the improvement of this system, that is, the complete design, production, and verification of the correct functionality of a completely new intelligent ultrasonic barrier guarding the entrance to the building through a door or gate.

2. Ultrasonic Barrier Demonstration

The entire ultrasonic barrier system is therefore intended for guarding access to a building or part of a building through a door or gate. To install the necessary components and to build the system and verify the correct function, a frame that enabled a simulation of the relevant entrance to a building was first made.

The frame of 2 m height and 1 m width was made of spruce wood beams. The barrier system consists of four bars that are 0.4 m apart, so that the entire area of the given passage is covered as evenly as possible. An illustrative picture together with an indication of the location of individual bars is shown in Fig. 1. The transmitting part in this case is on the left part of the frame and the receiving part is on the right part of the frame. Individual transmitting and receiving transducers are depicted by blue rectangles.

3. Construction of One Ultrasonic Bar

One ultrasonic bar of the whole system consists of a transmitter and a receiver block. The block diagram of the ultrasonic bar is shown in Fig. 2.

The transmitting part of the ultrasonic bar consists of a signal generator for piezoelectric ceramic transducer excitation, a piezoelectric ceramic transducer, and a power supply unit. An astable flip-flop circuit was implemented as the excitation signal generator for the piezoelectric

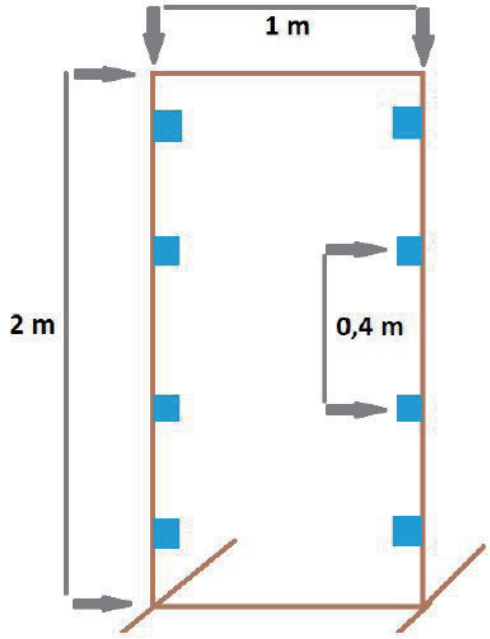

Fig. 1. (Color online) Frame made for system installation.

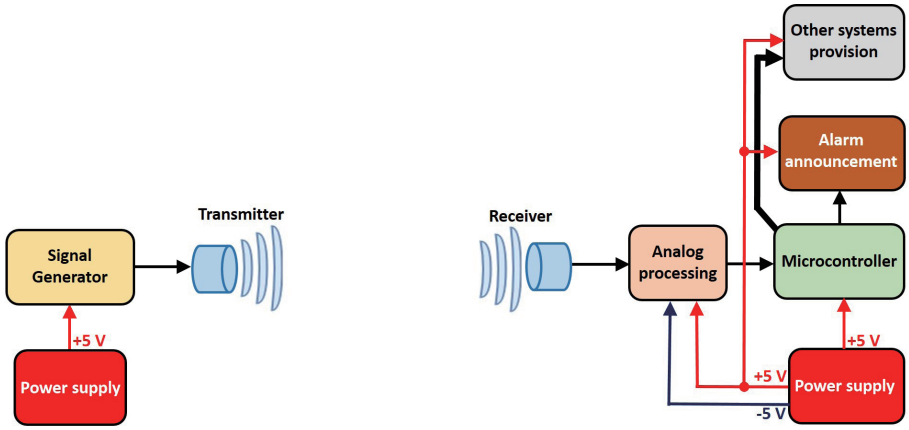

Fig. 2. (Color online) Block diagram of one ultrasonic bar.

ceramic transducer–transmitter using the NE555 integrated circuit from Texas Instruments Company.[29] The piezoelectric ceramic transducer marked MCUSD16A40S12RO from Multicomp Pro Company was used to convert the electrical signal into an acoustic signal.[30] This transducer works with the resonant frequency of 40 kHz and can be both a transmitter and a receiver.[30] The scheme of the excitation signal generator is shown in Fig. 3. Devices RA, Z3, RB, and C2 are very important in this circuit, because they set the parameters of the generated signal, especially the frequency. The range of the adjustable frequency of the generated signal

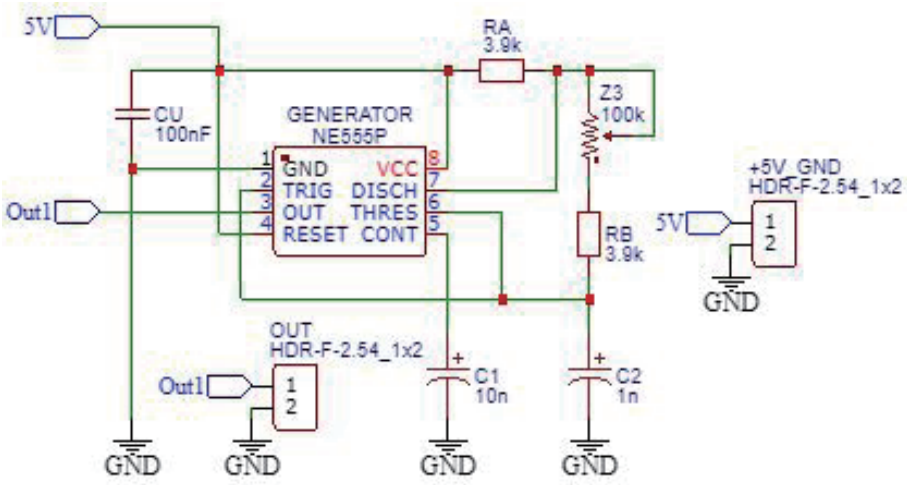

Fig. 3. (Color online) Scheme of excitation signal generator.

was chosen from 10 to 100 kHz owing to the future use of other transducers and also to the changing resonant frequency with temperature. The capacitance *C*2 was chosen to be 1 nF, the resistances *RA* and *RB* were chosen to be 3.9 kΩ, and the maximum resistance of the potentiometer *Z*3 was calculated to be 100 kΩ. The power supply for testing the correct functionality was solved using a laboratory power source.

The relation for calculating the frequency of the excitation signal is defined by Eq. (1):

$$f = 1.44/((RA + 2 \cdot (RB + Z3)) \cdot C2), \tag{1}$$

where *f* is the frequency of the excitation signal, *RA* is the resistance of the resistor RA, *RB* is the resistance of the resistor RB, *Z*3 is the resistance of the potentiometer Z3, and *C*2 is the capacitance of the capacitor C2.

The printed circuit board obtained by 3D simulation is shown in Fig. 4 on the left, and on the right is the real printed circuit board.

In Fig. 5, the waveform of the generated signal is shown. The waveform of the generated signal is therefore rectangular with a slight overshoot and a frequency of exactly 40 kHz. The possibilities of setting the signal frequency range of the manufactured generator were tested. Frequency adjustment was possible in the range from 6.6 to 98.3 kHz.

The reception part of the ultrasonic bar is much more sophisticated. The block diagram of the reception part of the ultrasonic bar is shown in Fig. 6.

As the receiving piezoelectric ceramic transducer, the same one as in the transmitting part was implemented. To amplify the signal from the piezoelectric ceramic transducer–receiver, a two-stage amplifier in an inverting circuit in the integrated device TL084CDT in the SOIC-14 package containing four operational amplifiers was used.[31]

The gain of both stages of this amplifier circuit is adjustable using VISHAY 64 Y potentiometers of 470 kΩ.[32] A two-way operational rectifier with the same operational amplifiers was used to remove the negative half-waves of the harmonic signal. To reduce the

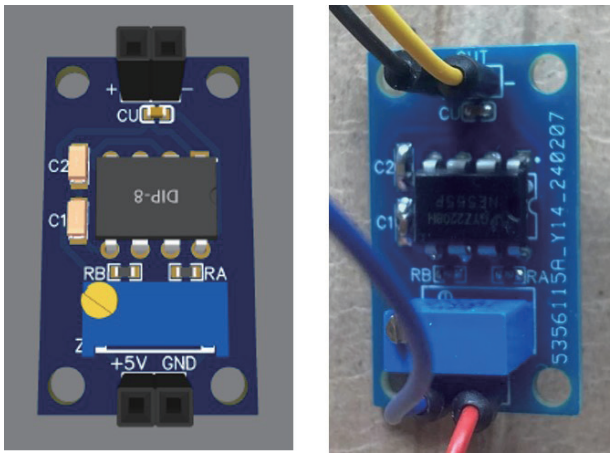

Fig. 4. (Color online) Printed circuit board of excitation signal generator.

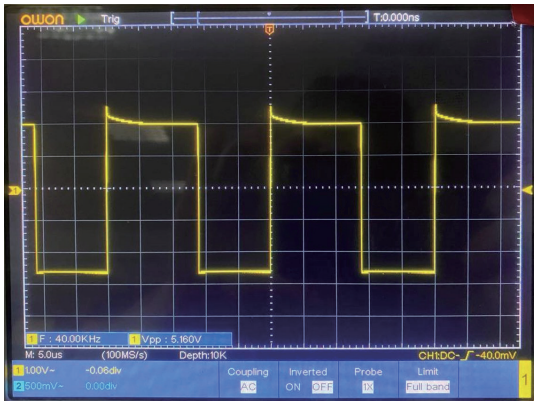

Fig. 5. (Color online) Waveform of generated signal.

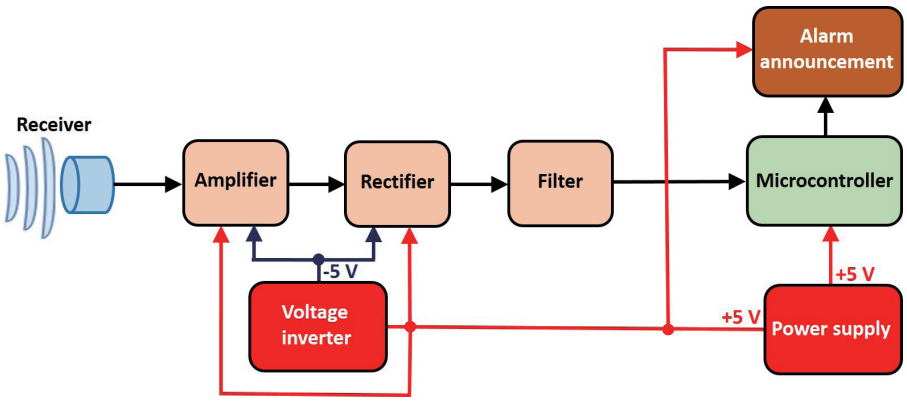

Fig. 6. (Color online) Block diagram of reception part of ultrasonic bar.

ripple of the output signal from the operational rectifier, a passive low-pass filter made of a ceramic capacitor with the capacity of 220 nF was used. This analogue preprocessed signal was fed to the input of the analogue-to-digital converter of the microprocessor system. The signal was subsequently digitally processed. An appropriate detection level has been set and alarm notification provided. The MH-EV LIVE ESP32 MiniKIT[33] with ESP-WROOM-32 module[34] was used as the microprocessor system. This module is powerful enough and enables wireless communication via Bluetooth, Bluetooth low energy, and Wi-Fi. Because of the possibility of wireless communication, availability, and low price, this module was chosen. For testing purposes, a laboratory power source was again used as the power supply system. For the analogue preprocessing of the output signal from the piezoelectric ceramic transducer–receiver, it was necessary to create a symmetrical power supply for the operational amplifiers. The ICL7660SCPAZ inverter from Renesas Electronics Company[35] was used for the negative branch of the supply voltage. The diagram of the analogue preprocessing of the output signal from the piezoelectric ceramic transducer–receiver is shown in Fig. 7.

The printed circuit board obtained by 3D simulation is shown in Fig. 8 on the left, and on the right is the real printed circuit board.

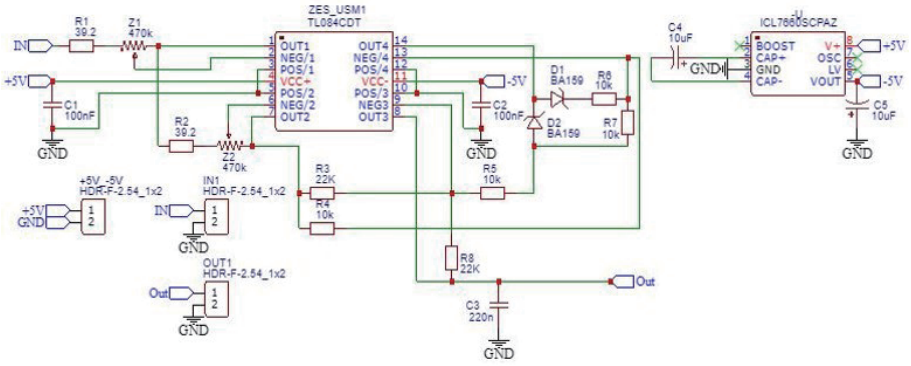

Fig. 7. (Color online) Scheme of analogue signal preprocessing from receiving transducer.

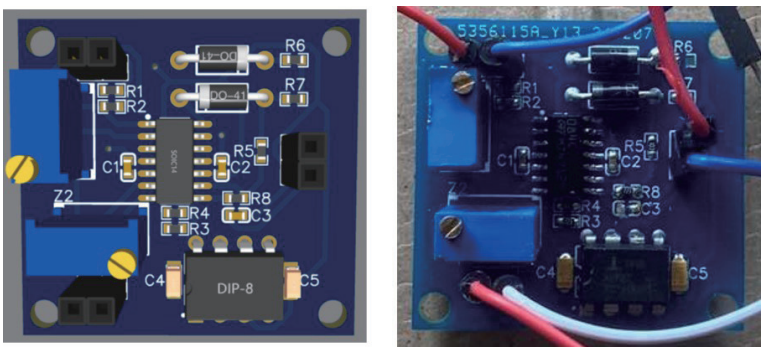

Fig. 8. (Color online) Printed circuit board of analogue signal preprocessing from receiving transducer.

An example of an analogue preprocessed signal before entering into the analog-to-digital converter of the microprocessor system is shown in Fig. 9.

The ripple of the analogue preprocessed signal in the range of minimum and maximum values is 360 mV, and the DC value is stabilized at 1.6 V. The implemented microprocessor system works with values in the range of 0–3.3 V, which the DC value of the input signal meets.

4. Construction of Complete Ultrasonic Barrier

Only the aforementioned piezoelectric ceramic transducers were installed in the vertical parts of the made frame. The signal generator and the evaluation system were attached to the lower part of the frame on the left and right sides. Individual piezoelectric ceramic transducers were connected to the aforementioned components via cables. The signal generator for exciting the piezoelectric ceramic transducers–transmitters was designed and manufactured from completely identical channels, as represented in Figs. 3 and 4. This generator contains six channels, which are here for the possible future implementation of vertical bars. The module for the analogue preprocessing of output signals from the piezoelectric ceramic transducers–receivers was assembled and manufactured also from identical channels, as shown in Figs. 7 and 8. This module contains four channels. The MH-EV LIVE ESP32 MiniKIT is attached to this module via connectors as the heart of the entire evaluation system. This microprocessor system evaluates the state of the ultrasonic barrier, determines the intruder, and provides information about the alarm. Information can be provided in three ways. A very simple way is using a piezoelectric siren and a LED, which is directly on the microprocessor system board. Another way is to display a short message on the monitor of a laptop computer. The laptop computer also provides system tuning and power supply to the evaluation part during tuning. The system can also work autonomously, and then wireless communication via Wi-Fi is used to inform about the

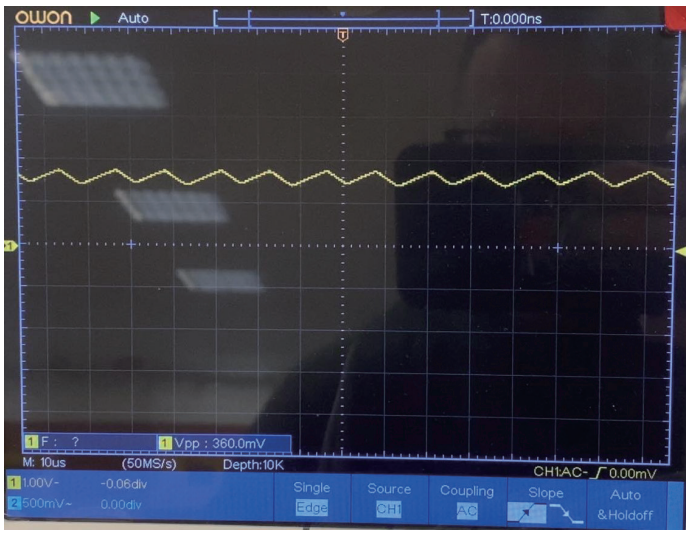

Fig. 9. (Color online) Analogue preprocessed signal.

presence of an intruder, when short messages about the intruder are transmitted. The power supply of the entire system in the case of its required autonomous function is provided by a network switching power supply with the voltage output of +5 V. The diagram of the complete system is shown in Fig. 10.

The printed circuit boards of the final components of the entire system are shown in Fig. 11. In the left part of the presented figure, there is the printed circuit board of a six-channel signal generator for piezoelectric ceramic transducers–transmitters obtained by 3D simulation and actually manufactured. The right part of the figure represents the module of the four-channel analogue preprocessing of signals from piezoelectric ceramic transducers–receivers obtained by 3D simulation and actually manufactured. The aforementioned microprocessor system is inserted into this module using the appropriate connectors, which is at the center of Fig. 11.

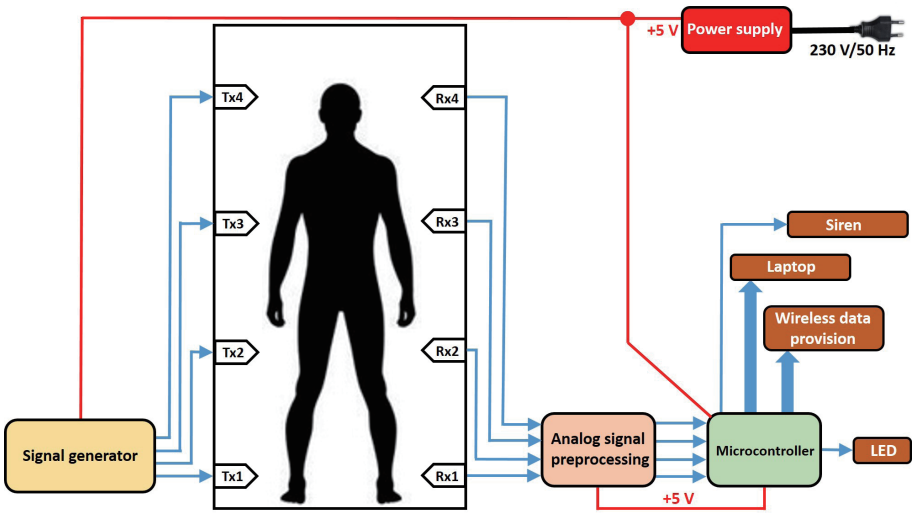

Fig. 10. (Color online) Scheme of entire system.

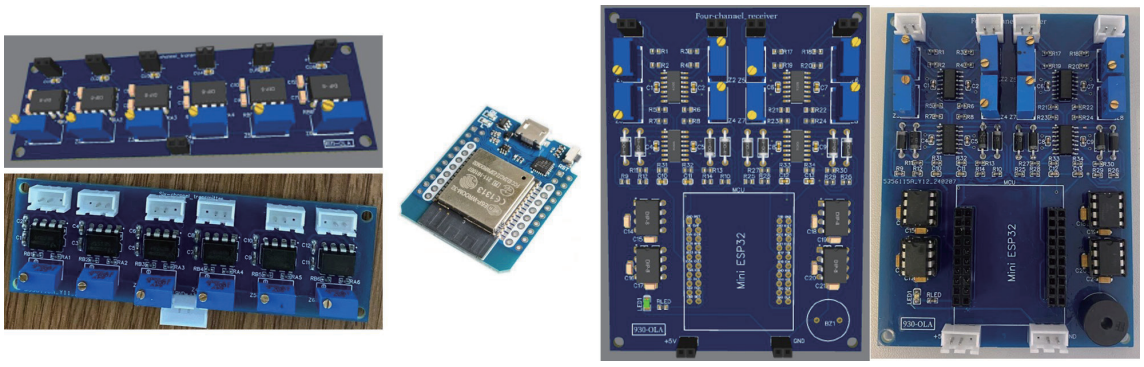

Fig. 11. (Color online) Printed circuit boards of final components of entire system.

5. Algorithm in Microprocessor System

The algorithm in the microprocessor system therefore solves the conversion of the analogue preprocessed signal from piezoelectric ceramic transducers–receivers into digital form, determines the detection values of individual ultrasonic bars, evaluates the status of individual bars, detects the presence of an intruder and the type of intrusion of the entire barrier, and ensures the signaling of the intrusion and the provision of information about the intrusion wirelessly via Wi-Fi to a remote station. The flowchart of the complete algorithm is shown in Fig. 12.

After turning on the system or a possible reset of the microprocessor, four inputs are set for individual bars, the output for the LED and acoustic piezoelectric siren is set, the serial line configuration for diagnostic messages during system debugging is set, and necessary variables are declared and set to zero, with which the algorithm subsequently works. The baud rate at which communication is carried out over the serial line was chosen to be 115200 bps. Next comes a loop in which the following program structures are constantly repeated. The output from the analogue signal preprocessing block for individual bars is read and converted into digital form, and the adequate voltage is calculated. For the stability of the voltage, filtering is performed using a moving average. A different number of moving average samples were used for each bar. This was determined by testing. The optimal number of samples was determined so that the voltage would be sufficiently stable and the calculation would not be very long. A larger

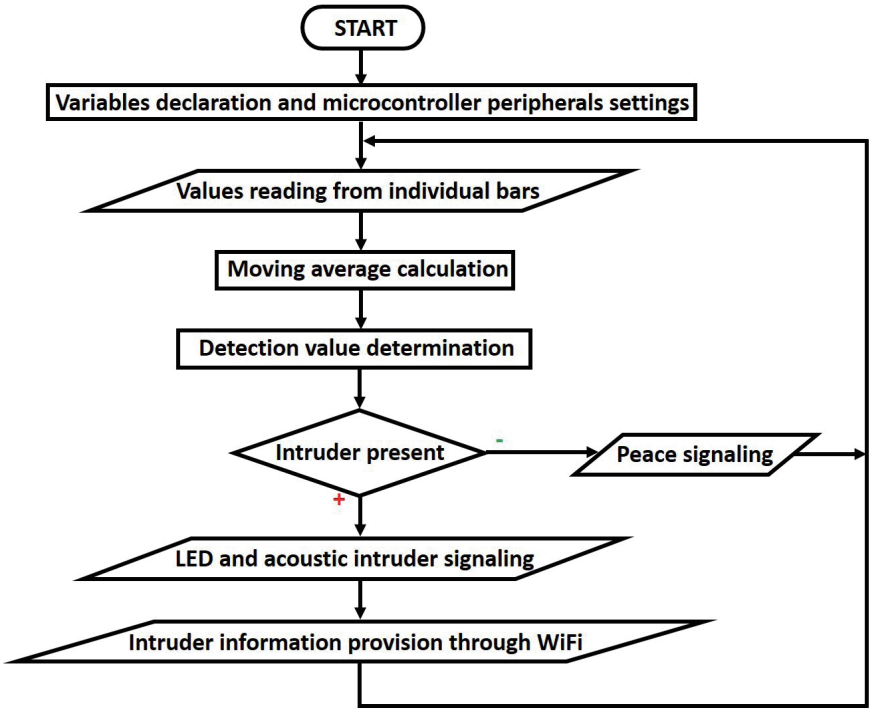

Fig. 12. (Color online) Algorithm flowchart in microprocessor system.

number of samples for calculating the moving average may reduce the speed of intruder detection. Thus, the number of samples was set at 20 for the upper and lower bars and 24 for the two middle ones. This was followed by determining the voltage in the absence of an intruder. The value differed again among individual bars. This may be due to losses in the cabling, the installation of individual transducers, which could cause a slight deviation from the axis, a slight difference in resonant frequency among individual transducers, and also differences in the settings of the transfer size of individual amplification stages. The individual detection levels were determined at the following voltages: upper bar, 0.88 V; two middle ones, 0.97 V; and lower bar, 1.13 V. Thus, when these values are measured on individual bars, peace is signaled. If the values are zero, an alarm signal is generated via the LED and acoustically, and also by sending a short message wirelessly via Wi-Fi. The entire ultrasonic barrier system has been given a certain intelligence, which can valuate both the alarm and the type of intruder. It evaluates the individual alarm states on the bars and determines the type of intruder on the basis of their combination. Four bars are implemented, so there are 16 states with certain results, which are shown in Table 1.

There are therefore four types of the most probable intruder defined here, namely, a person, an animal, a child, and a flying object, which are determined according to the combinations of the logical values of the individual bars. Logical 1 corresponds to the presence of an intruder. There are combinations that are not entirely probable. There, a barrier intrusion and an unwanted alarm are signaled. If all the bars are in logical 0, no barrier intrusion is evaluated and peace is signaled. It is assumed here that the transmission and reception of the signal work without problems.

Table 1
Combination of states on the individual bars and corresponding situations.

R × 4	R × 3	R × 2	R × 1	Situation, intruder type
0	0	0	0	Peace
0	0	0	1	Animal
0	0	1	0	Barrier intrusion, flying object
0	0	1	1	Child, larger animal
0	1	0	0	Barrier intrusion, flying object
0	1	0	1	Barrier intrusion, unwanted alarm
0	1	1	0	Flying object
0	1	1	1	Person
1	0	0	0	Barrier intrusion, flying object
1	0	0	1	Barrier intrusion, unwanted alarm
1	0	1	0	Barrier intrusion, unwanted alarm
1	0	1	1	Barrier intrusion, unwanted alarm
1	1	0	0	Flying object
1	1	0	1	Barrier intrusion, unwanted alarm
1	1	1	0	Person
1	1	1	1	Person

6. Functionality Verification of Entire System

The verification of the functionality of the complete ultrasonic barrier system was carried out under laboratory conditions at the temperature of 22 ℃. The verification of functionality was mainly focused on evaluating individual alarm states. After connecting the individual components, the transmitting and receiving parts of the barrier were finally tuned, and the functionality and signaling of the peace state in the absence of an intruder were examined. The system worked without problems and the peace state was signaled. Subsequently, the ability to evaluate and send the signal of the individual types of intruder was tested. The individual tests are shown in Fig. 13 in cascaded images next to each other. Here, a soldier (co-author of this article) played the role of individual intruders in the simulation and performed the tests.

First, a person passing through the barrier was tested. This was followed by a test of a small animal passing through. The next test was the intrusion of the barrier by a child or a larger animal. The penultimate test was a flying object. The flying object was simulated here by throwing a military clothing through the barrier. The last was a test of one of the unlikely states on the barrier, namely, the intrusion of one of the bars, in this case, the upper one, which could also simulate a flying object or any barrier intrusion. Each test was performed 10 times and the system always correctly detected the presence and type of intruder. Furthermore, in the case of any intruder, i.e., a person, both fast and slow passage were tested. During slow passage, it was very clear how the detection gradually comes out from the individual bars in the barrier. During fast passage, the detection by individual bars was not clearly visible; however, the system signaled the alarm overall correctly. This showed that the system is capable of detecting even a fast-moving person, animal, and actually any flying object, and raising an alarm when they enter into the guarded area.

Fig. 13. (Color online) Demonstration of individual tests.

7. Conclusions

In this article, we presented the detailed design and description of a manufactured and functional barrier system that uses ultrasonic technology. As transmitters and receivers, piezoelectric ceramic transducers in an air-to-air configuration are implemented here, which are very easily available on the market of electrical components, and therefore not very economically demanding. The signal generator used for exciting the piezoelectric ceramic transducers–transmitters was the astable flip-flop circuit with a rectangular output waveform. This method was chosen as the simplest way of generating the excitation signal for this transducer. Given that the mentioned transducers are narrowband, this signal is sufficient. A modern microprocessor system was used for digital signal processing and the evaluation of the presence and type of intruder. The great advantage of this module is that it enables wireless communication via Bluetooth, Bluetooth low energy, and Wi-Fi, and sends information about the intruder to a remote station. With these technologies, the microprocessor system can also be reprogrammed remotely. The system was given a certain intelligence, which can recognize the type of intruder.

The designed, manufactured, and assembled ultrasonic barrier represents an improvement of the prototype, which can be significantly modified in the future. The first modification could be the design of a more sophisticated excitation generator for piezoelectric ceramic transducers–transmitters. The improvement would consist of the design of a harmonic signal generator, which would be suitably modulated and controlled by a microprocessor system for resistance to attempts at sabotage and deception of the system. This would then lead to different analogue preprocessing and digital processing on the receiving side. The next improvement could be microprocessor-controlled amplification in the analogue signal preprocessing part. Owing to this, the optimal transmission of individual bars would be automatically set during the initial installation and tuning of the system. Another modification could be the addition of vertical bars to the system, thus creating a curtain and increasing the sensitivity of detection. The last improvement to the system could be the addition of a global system for a mobile communication module for transmitting messages about an intruder over significantly greater distances.

Acknowledgments

The work presented in this article was supported by the Czech Republic Ministry of Defence – University of Defence Development Program – “Conduction of Operations in Airspace”.

References

1 Z. Li, X. Yang, H. Lan, M. Wang, L. Huang, X. Wei, G. Xie, R. Wang, J. Yu, Q. He, Y. Zhang, and J. Luo: Ultrasonics **143** (2024) 1. https://doi.org/10.1016/j.ultras.2024.107409
2 H. Hu, Ch. Hu, W. Guo, B. Zhu, and S. Wang: Ultrasonics **142** (2024) 1. https://doi.org/10.1016/j.ultras.2024.107401
3 Ch-H. Lin, M-Ch. Ho, P-Ch. Lee, P-J. Yang, Y-M. Jeng, J-H. Tsai, Ch-N. Chen, and A. Chen: Ultrasonics **142** (2024) 1. https://doi.org/10.1016/j.ultras.2024.107391
4 X. Su, Y. Wang, H. Chu, L. Jiang, Y. Yan, X. Quiao, J. Yu, K. Guo, Y. Zong, and M. Wan: Ultrasonics **142** (2024) 1. https//doi.org/10.1016/j.ultras.2024.107379

5 C. O. Manlises, J-W. Chen, and Ch-Ch. Huang: Ultrasonics **141** (2024) 1. https://doi.org/10.1016/j.ultras.2024.107320
6 Y. Gou, Y. Yan, Y. Lyu, S. Chen, J. Li, and Y. Liu: Ultrasonics **142** (2024) 1. https://doi.org/10.1016/j.ultras.2024.107400
7 D. Sun, W. Zhu, Y. Xiang, and F-Z. Xuan: Ultrasonics **142** (2024) 1. https://doi.org/10.1016/j.ultras.2024.107356
8 Ch. Ma, J. Liu Z. Cui, and T. Kundu: Ultrasonics **142** (2024) 1. https://doi.org/10.1016/j.ultras.2024.107357
9 L. Littner, I. Solodov, and M. Kreutzbruck: Ultrasonics **142** (2024) 1. https://doi.org/10.1016/j.ultras.2024.107373
10 Z. Wang, X. Li, Y. Liu, Y. Lv, and M. Li: Ultrasonics **142** (2024) 1. https://doi.org/10.1016/j.ultras.2024.107381
11 H. Chen and J. Tao: Ultrasonics **142** (2024) 1. https://doi.org/10.1016/j.ultras.2024.107382
12 Y. Qiu, Y. Jiang, B. Wang, and Z. Huang: IEEE Sens. Lett. **5** (2023) 1. https://doi.org/10.1109/LSENS.2023.3267278
13 A. Hashmi and A. N. Kalashnikov: Ultrasonics **99** (2019) 1. https://doi.org/10.1016/j.ultras.2019.105969
14 A. R. Patkar and P. P. Tasgaonkar: Proc. Int. Conf. Communication and Signal Processing (2016) 983–986. https://doi.org/10.1109/ICCSP.2016.7754294
15 S. Kim and H. Kim: Int. J. Control, Autom. Syst. **8** (2010) 1280. https://doi.org/10.1007/s12555-010-0613-x
16 S. Kim, J. Jang, and H. B. Kim: Proc. 7th Int. Conf. Informatics in Control, Automation and Robotics (2010) 340–343. https://doi.org/10.5220/0002878803400343
17 Ch-Y. Lee, H-G. Choi, J-S. Park, K-Y. Park, and S-R. Lee: Proc. IEEE Sensors (IEEE, 2007) 985–988. https://doi.org/10.1109/ICSENS.2007.4388569
18 Y. Arai, H. Asama, H. Kaestsu, and I. Endo: Distance Measurment in Multi-Robot Systems based on Time Shared Scheduling, in Distributed Autonomous Robotic Systems 4, Springer Nature (Tokyo, 2000) pp. 189–198. https://link.springer.com/chapter/10.1007/978-4-431-67919-6_18
19 R. J. Przybyla, S. E. Shelton, C. Lee, B. E. Eovino, Q. Chau, and M. H. Kline: Proc. 36th Int. Conf. Micro Electro Mechanical Systems (IEEE, 2023) 961–964. https://doi.org/10.1109/MEMS49605.2023.10052367
20 B. T. Sturtevant, N. Velisavljevic, D. N. Sinha, Y. Kono, and C. Pantea: Rev. Sci. Instrum. **7** (2020) 1. https://doi.org/10.1063/5.0010475
21 R. C. Mayworm, A. V. Alvarenga, and R. P. B. Costa-Felix: Physics Procedia **70** (2015) 590. https://doi.org/10.1016/j.phpro.2015.08.029
22 D. Grimaldi: Proc. Second IEEE Int. Workshop Intelligent Data Acquisition and Advanced Computing Systems: Technology and Applications (IEEE, 2003) 365–370. https://doi.org/10.1109/IDAACS.2003.1249588
23 R.Sharma, K. S. Dhingra, N. Pandey, R. Garg, and R. Singhal: Proc Int. Conf. Intelligent Systems, Modelling and Simulation (2010) 423–426. https://doi.org/10.1109/ISMS.2010.82
24 O. Sonbul and A. N. Kalashnikov: Proc. 7th Int. Conf. Intelligent Data Acquisition and Advanced Computing Systems (IEEE, 2013) 235–238. https://doi.org/10.1109/IDAACS.2013.6662679
25 Y.-W. Bai, Z-H. Li, and Z-L. Xie: Proc. IEEE Int. Symp. Consumer Electronics (IEEE, 2010) 1–6. https://doi.org/10.1109/ISCE.2010.5522729
26 M. L. Garcia: The Design and Evaluation of Physical Protection Systems (Burlington, USA: Butterworth-Heinemann, 2008) 2nd ed. https://www.sciencedirect.com/book/9780750683524/design-and-evaluation-of-physical-protection-systems
27 M. L. Garcia: Vulnerability Assessment of Physical Protection Systems (Burlington, USA: Butterworth-Heinemann, 2006). https://shop.elsevier.com/books/vulnerability-assessment-of-physical-protection-systems/garcia/978-0-7506-7788-2
28 P. Janů and B. Odvárková: J. Electr. Eng. **5** (2022) 343. https://doi.org/10.2478/jee-2022-0046
29 xx555 Precision Timers: https://docs.rs-online.com/ae11/A700000009214226.pdf (accessed October 2025).
30 Ultrasonic Sensor: https://www.farnell.com/datasheets/3771810.pdf (accessed October 2025).
31 TL084, TL084A, TL084B: https://img.eecart.com/dev/null/TL084ID-STMicroelectronics.pdf (accessed October 2025).
32 3/8" Square (10 mm) Multi-Turn Cermet Trimmer: https://www.vishay.com/docs/51026/t93.pdf (accessed October 2025).
33 RIOT OS MH-ET LIVE MiniKit: https://doc.riot-os.org/group__boards__esp32__mh-et-live-minikit.html#details (accessed October 2025).
34 ESP32-WROOM-32: https://www.espressif.com/sites/default/files/documentation/esp32-wroom-32_datasheet_en.pdf (accessed October 2025).
35 ICL7660S, ICL7660A Super Voltage Converters: https://www.renesas.com/en/document/dst/icl7660s-icl7660a-datasheet?srsltid=AfmBOorHy2gnCDbtdT8TL-rq1tCIjRJbrxqbCfcLQgF4AkvW3wVqeNg2 (accessed October 2025).

About the Authors

Přemysl Janů was born in 1982 in Šternberk, Czech Republic. He received his M.Sc. degree in special equipment of aircraft in 2006 and his Ph.D. degree in electrical systems and devices in 2011 from the University of Defence in Brno, Czech Republic. He is currently Head of Group of Avionics and Aircraft Armament Systems at the Department of Aviation Technology, Faculty of Military Technology, University of Defence, Czech Republic. His current research interests include piezoelectric ceramic transducers, the electrical equivalent definition and simulation of a response on an input signal, sensor technology, sensor signal processing, and inertial navigation systems.

Antonín Kučera was born in 1998 in Olomouc, Czech Republic. He received his M.Sc. degree in radar technology and electronic warfare in 2024 from the University of Defence, Czech Republic. He is currently an officer at the Operational Analysis Workplace at Passive Surveillance System Company, Tábor, Czech Army Ground Forces. His research interests include radar technology, electronic warfare, electronic security systems, sensors, and sensor signal processing.